Contract No:

This document was prepared in conjunction with work accomplished under Contract No. 89303321CEM000080 with the U.S. Department of Energy (DOE) Office of Environmental Management (EM).

Proceedings of the ASME 14th International Pipeline Conference
IPC2022
September 26 - 30, 2022, Calgary, Alberta, Canada

[redacted]

IPC2022-86927

IMPROVED FRACTURE TOUGHNESS TEST METHOD FOR SINGLE EDGE NOTCHED TENSION SPECIMENS IN CLAMPED-END CONDITIONS

Xian-Kui Zhu
Materials Technology
Savannah River National Laboratory
Aiken, South Carolina 29808, USA

ABSTRACT

The oil and gas industry has favored to use fracture toughness measured using single edge-notched tension (SENT) specimen in the clamped-end conditions for the strain-based design or fitness for service analysis of pipelines. Different SENT fracture test methods have been developed, including DNV, CANMET and ExxonMobil procedures in terms of the J-integral or crack tip opening displacement (CTOD). These efforts led to the first SENT test standard BS 8571 published.

However, these SENT methods may determine inconsistent test results on fracture toughness for the same specimen because no consensus is reached for any of the methods, and different estimate equations are used for an experimental evaluation. This paper aims to develop an improved SENT fracture toughness test method after a comparative study on the primary SENT fracture test methods. Comparisons are performed on available solutions of the stress intensity factor K, the geometrical eta factor, the elastic compliance inverse equation, and the m factor for converting the J-integral to CTOD that all were obtained for the clamped SENT specimens. Through comparisons, this work identified a set of more accurate solutions for the K factor, the eta factor, the compliance equation, the m factor, and those used for weld testing. The difference between the J-converted CTOD and double clip gage measured CTOD is also discussed. On these bases, an improved SENT test method is proposed for determining more reliable fracture toughness or resistance curves for ductile pipeline steels.

KEYWORDS: CTOD, J-integral, double clip gage, R-curves, fracture toughness, SENT specimens

1. INTRODUCTION

In the oil and gas industry, the pipeline integrity assessment requires fracture toughness in a fracture mechanics analysis. Fracture toughness is an important material property and characterized by different fracture parameters, including the stress intensity factor K proposed by Irwin [1] for brittle materials and the J-integral proposed by Rice [2] or crack tip opening displacement (CTOD) proposed by Wells [3] for ductile materials. Those fracture parameters can effectively describe both material toughness and crack driving force for a structure containing cracks. They have been widely applied to material selection, crack assessment, engineering critical analysis (ECA) or fitness for service (FFS) analysis [4-5] for pressure vessels and oil/gas pipelines. Over the past half century, many efforts have been made worldwide to develop effective fracture test methods and standards, as reviewed by Zhu and Joyce [6]. To obtain conservative fracture toughness, the bending dominant fracture specimens with high constraint were adopted in the standard fracture test methods developed by the American Society for Testing and Materials (ASTM), British Standard Institution (BSI) or other international organizations. The most often used standard specimens are compact tension (CT) and single edge notched bend (SENB) specimens with deep cracks (a/W>0.45). Application showed that the standard fracture toughness measured using CT or SENB works well in the fracture mechanics analysis, but can be overly conservative for shallow cracks in the real world due to the low-constraint effects. Thus, different fracture test methods in the low-constraint conditions have been developed for determining more realistic and less conservative fracture toughness, as recently reviewed by Zhu [7]. It includes the semi-analytical fracture constraint correction

This work was produced by Battelle Savannah River Alliance, LLC under Contract No. 89303321CEM000080 with the U.S. Department of Energy. Publisher acknowledges the U.S. Government license to provide public access under the DOE Public Access Plan (http://energy.gov/downloads/doe-public-access-plan).

method [8] and direct fracture test methods using different low-constraint, nonstandard fracture test specimens.

Over the past 20 years, several direct fracture test methods have been developed in the oil and gas industry for determining less-conservative fracture toughness or resistance curves in terms of the J-integral or CTOD using single edge-notched tension (SENT) specimens in the clamped-end conditions. Such fracture toughness has been shown adequate to use for assessing shallow cracks in oil/gas pipelines, leading to a great cost saving in the pipeline integrity management. Recently, a technical review of SENT fracture toughness testing was given by Zhu et al. [9-10], where three typical industrial practices of SENT testing were discussed, including the DNV [11], CANMET [12-13] and ExxonMobil [14-15] methods for the J-integral, J-R or CTOD-R curve testing. While the DNV practice was developed for the multiple-specimen tests, the CANMET and ExxonMobil methods were developed for the single-specimen test. Based on these efforts, BSI published the first SENT test standard with a designation of BS 8571 [16] in 2014 and updated in 2018.

In contrast to BSI, ASTM has not accepted SENT as a standard specimen yet because there is no consensus so far from the standard development organizations. Nevertheless, ASTM is making ongoing efforts for developing a robust test method for SENT specimens after obtaining a strong consensus in the near future. For this end, a special issue on SENT fracture toughness testing and its applications to high-strength pipeline steels was recently published by two guest editors: Dr. Zhu and Mr. Weeks [17] in International Journal of Pressure Vessels and Piping (IJPVP) in Vol. 156, 2017. This special issue contains eight high-quality papers on the SENT test method, test procedure, experimental evaluation, data validation, and current challenge for obtaining a reliable SENT test method for ASTM. Detailed discussions can be found in the journal.

In the special issue of IJPVP, the present author [10] delivered a comprehensive technical review on existing SENT fracture test methods with a focus on experimental evaluation using the DNV practice, CANMET method, ExxonMobil method and BS 8571 standard as well as recent progresses. While better agreements have been observed for the J-R curve testing, significant differences remain for the CTOD testing due to the J-conversion and double clip gage (DCG) measurement methods, in addition to other challenges. So motivated, this paper performs a comparative study on primary available fracture test methods using the clamped SENT specimens, and an improved SENT fracture toughness test method is developed.

2. REVIEW OF EXISTING SENT TEST METHODS

Recently, Zhu [10] delivered a comprehensive technical review of the SENT test methods for the J-integral and CTOD testing with clamped SENT specimens. It includes development and progress in SENT fracture toughness testing, experimental evaluation of J-R curves and CTOD-R curves, advantages and disadvantages, test procedures and experimental estimate equations for SENT fracture testing. A brief review of primary existing SENT test methods is presented next.

2.1 The J-Integral Test Method

The clamped SENT specimen is considered in this work, as shown in Fig. 1, where the specimen width is denoted as W, the daylight length is H=10W, and the clamped area at each end has a griping length of 4W, leading to a total specimen length of 18W. The single specimen test method is discussed in this work, and the multiple specimen test method developed by DNV [11] is not discussed. For the clamped SENT specimens, CANMET [12-13] developed their single specimen test procedure by following the guideline in ASTM E1820 [18] for both J-R curve and CTOD-R curve testing, where the J-integral converted CTOD test method developed in ASTM E1820 [18] was adapted by CANMET for the SENT CTOD testing.

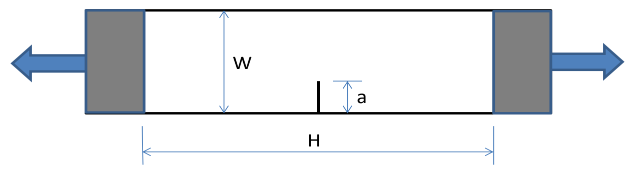

Figure 1. Schematic diagram of a clamped SENT specimen

As used in ASTM E1820 [18], the J-integral is usually separated into an elastic component and a plastic component, and calculated under plane strain conditions at a given loading level:

$$J = J_{el} + J_{pl} \tag{1}$$

where the elastic component J_{el} is calculated from the stress intensity factor K by $J_{el}=K^2/(E/(1-\nu^2))$ with Young modulus E and Poison ratio ν, and the plastic component J_{pl} is determined using the η factor and the plastic area from the applied force versus crack-mouth opening displacement (CMOD) curve

$$J_{pl} = \frac{\eta_{CMOD} A_{pl}}{B\,b} \tag{2}$$

where B is the specimen thickness, b=W-a is the ligament size, W is the specimen width, a is the crack length, η_{CMOD} is the CMOD-based geometrical factor, and A_{pl} is the area of the applied force versus plastic CMOD measured in testing.

Equation (2) is typically used for stationary cracks or the basic method of the J-R curve testing. The elastic compliance equation and the K factor solution were numerically obtained by CANMET [12-13]. More accurate expressions of the K factor were recently obtained by Zhu [19-20].

For a quasi-static growing crack, Eq. (2) cannot be directly used without consideration of crack growth correction on the J-integral. For the single specimen test, after consideration of crack growth correction, Eq. (2) is replaced by the incremental J-integral equation developed by Zhu et al. [21] in 2007 and adopted by ASTM E1820 [18] since 2008:

$$J_{pl(i)} = \left(J_{pl(i-1)} + \frac{\eta_{CMOD}^{i-1}}{b_{i-1}B_N} A_{pl}^{i-1,i}\right)\left(1 - \frac{\gamma_{CMOD}^{i-1}}{b_{i-1}}(a_i - a_{i-1})\right) \tag{3}$$

where a_{i-1} and b_{i-1} are crack length and ligament size at the (i-1)th load step, B_N is the net thickness of side-grooved specimen, η_{CMOD} and γ_{CMOD} are two CMOD-based plastic geometrical factors in a function of *a/W*, $A_{pl}^{i-1,i}$ is the incremental plastic area under the load-CMOD curve, and CMOD is measured using a single clip gage mounted on the crack mouth of specimen. In ASTM E1820 [18], the unloading compliance method was recommended for measuring crack extension. The J versus Δa (=a_i-a_0) relation is called J-R curve and used to characterize fracture resistance during stable crack tearing.

CANMET [12-13] adopted the incremental J-integral equation (2) in their SENT test procedure to determine J-R curves on a single SENT specimen test. By use of the plane strain elastic-plastic finite element analysis (FEA), they obtained the numerical results of the two geometrical factors η_{CMOD} and γ_{CMOD} used in Eq. (2) as a function of a/W.

In addition to CANMET, University of Sao Paulo (USP) [22-23] also employed the incremental J-integral equation (3) in their SENT test procedure to determine J-R curves on a single specimen test, where the unloading compliance method was used to measure crack extensions. Using the FEA simulations, they obtained different results of the K factor, the factor η_{CMOD} and γ_{CMOD}, and the CMOD compliance equation.

Equations (1) to (3) show that determining a reliable J-R curve depends on accurate experimental measurements of applied force P and CMOD, crack extension estimation and the J-integral calculation. This requires an accurate equation for the K factor, the geometrical factors η_{CMOD} and γ_{CMOD}, and the elastic compliance equation in an experimental evaluation. These four quantities will be discussed latter in detail.

2.2 The J-Integral Converted CTOD Method

CANMET [12-13] adopted the J-integral conversion method used in ASTM E1820 [18] to calculate CTOD from the J-integral for cracks in a single-specimen SENT test:

$$CTOD = \frac{J}{m\sigma_Y} \quad (4)$$

where the effective yield stress $\sigma_Y = (\sigma_{ys} + \sigma_{uts})/2$, σ_{ys} is the yield stress, σ_{uts} is the ultimate tensile stress (UTS), and *m* is a constraint factor in a function of *a/W* and strain hardening rate. Note that the *m* factor was determined from the FEA calculations with CTOD defined by the 90º interception approach for stationary cracks. The CTOD - *Δa* relation is called CTOD-R curve and serves as an alternative mean to characterize fracture resistance during stable crack tearing.

Equation (4) shows that in the J-integral conversion method, determination of an accurate CTOD depends on the accuracy of the m factor solution. Based on the plane strain elastic-plastic FEA calculations for the clamped SENT specimens with a square cross section, Shen and Tyson [24] obtained a curve-fit relation of the *m* factor in Eq. (4) as a function of the applied force P, crack size a/W and material strain hardening exponent N:

$$m = \begin{cases} m_c, & P \le P_Y \\ m_c - m_p\left(\frac{P}{P_y} - 1\right), & P > P_Y \end{cases} \quad (5)$$

where *P* is the applied force, $P_Y = B_N b \sigma_Y$ is the limit load of the clamped SENT specimen, two parameters m_c and m_p are expressed in a function of *a/W* and strain hardening exponent *N* of an elastic-power law material:

$$\begin{cases} m_c = A_1\frac{a}{W} + A_2 \\ m_p = B_1\frac{a}{W} + B_2 \\ A_1 = -0.1293 + 0.1152N - 0.00986N^2 + 0.000263N^3 \\ A_2 = 3.0867 - 0.297N + 0.0194N^2 - 0.000427N^3 \\ B_1 = 1.0169 - 0.0634N + 0.00567N^2 - 0.000200N^3 \\ B_2 = 0.6969 - 0.1216N + 0.01487N^2 - 0.000393N^3 \end{cases} \quad (6)$$

where the m factor is valid for 0.2≤a/W≤0.5 and 5≤N≤20. Note that CANMET considered the loading effect on the m factor. Similarly, Huang and Zhou [25] obtained another curve-fit function of the m factor, with loading level quantified by CMOD, rather than the applied force. These two expressions of the m factor are very complicated in a function of a/W, N and loading level, thus their applications are limited [10].

In addition, a loading-independent expression of the m factor was proposed by many other investigators [26-28]. After analyzing the available expressions of the m factor, Zhu [10] pointed out that further study is still needed to determine a more accurate m expression for SENT specimens. Presently, Zhu [10] and Ruggieri [28] suggested that the following m factor obtained recently by Sarzosa et al. [27] at USP should be used in the J-converted CTOD calculation:

$$m = 1.1171 - 0.2777\left(\frac{a}{W}\right) + 0.2218\left(\frac{a}{W}\right)^2 + 3.482\frac{1}{N} - 0.0012N + 1.6911SG - 1.1942SG^2 \quad (7)$$

where the *m* factor above is valid for 0.2≤a/W≤0.7, 5≤N≤20, and 0<SG=1-B_N/B≤0.2. This m expression was curve-fit from the 3D FEA results of side-grooved (SG) SENT specimens.

2.3 Double Clip Gage Measured CTOD Method

In contrast to the J-integral conversion method, ExxonMobil [14-15] proposed a simple, direct CTOD measurement method for the single SENT specimen test. They adopted a DCG measurement technique, where two clip gages were mounted on the crack mouth of a clamped SENT specimen with two heights of gage clip knifes. In reference to the linear extrapolation technique, CMOD and CTOD are simply calculated from the DCG measured displacements at the two knife heights by:

$$CMOD = V_1 - \frac{h_1}{h_2 - h_1}(V_2 - V_1) \quad (8)$$

$$CTOD = V_1 - \frac{h_1 + a_0}{h_2 - h_1}(V_2 - V_1) \quad (9)$$

where CTOD is defined at the original crack tip, V_1 and V_2 are displacements measured by the two clip gages at two knife heights h_1 and h_2 above the specimen front surfaces. Technically, extrapolation is less accurate than interpolation. The CMOD point is very close to the V_1 location (h_1=2 mm), but the crack-tip point is much further than h_1, and thus CMOD in Eq. (8) is more accurate than CTOD in Eq. (9). Moreover, an extrapolated CTOD is accurate only if the actual CTOD at the original crack tip is on or closer to the extrapolated straight line from the two measured displacements at the two clip knife locations.

In addition to ExxonMobil, Ghent University (UGent) [29] developed another experimental guideline to determine CTOD-R curves for clamped SENT specimens. They defined a slightly different CTOD using the 90°-interception approach at the original crack tip to calculate CTOD and CMOD for a growing crack, and the crack extension was monitored using the direct current potential drop (DCPD) method. Experimental results of Zhu et al. [30] showed that the CTOD-R curves determined using the ExxonMobil and UGent methods have small differences.

2.4 The CTOD test method in BS 8571

In the SENT test standard BS 8571 [16], the DCG method was adopted for determining CTOD and its R-curve from a single specimen test. In the evaluation of CTOD-R curve, total CTOD is separated into elastic and plastic parts. The elastic CTOD is calculated from the stress intensity factor K, and the plastic CTOD is determined from plastic components of DCG measured displacements. As a result, using DCG measured displacements, the total CTOD is calculated by:

$$CTOD = \frac{K^2}{2\sigma_{ys}E'} + \left[V_{p1} - \frac{a_0 + z_1}{z_2 - z_1}\left(V_{p2} - V_{p1}\right) \right] \quad (10)$$

where V_{p1} and V_{p2} are plastic components of the clip gage displacements measured at two knife heights z_1 and z_2. Typically, the knife heights z_1=2 mm and z_2=8 mm are recommended in the DCG arrangement [14-15]. With the initial compliance C_0, plastic displacement V_p=V-C_0P. Note that the DCG measured CTOD in Eq. (9) or (10) is defined at the original crack tip, whereas the J-converted CTOD is defined at the blunting crack tip using the 90°-intercept approach. Although the definitions are different, the two CTOD-R curves are comparable during crack blunting and at small crack extensions.

3 COMPARISONS OF EXISTING SENT TEST METHODS

This section reports the progress in development of SENT fracture toughness test methods and evaluates those test methods through comparison of typical results with a goal to achieve a consensus towards developing an improved test method for clamped SENT specimens. This work focuses on the latest results of the K factor, two η factors, the m factor, and the CMOD elastic compliance equation. Difference between the two CTOD methods is discussed using experimental examples for the clamped SENT specimens in different ductile steels.

3.1 Stress Intensity Factor

There are two numerical solutions of the K factor obtained by CANMET [12] and USP [22] and a complex analytical K solution obtained by Ahmad et al. [31]. BS 8571: 2014 [16] utilized the simple CANMET K solution for non-wide SENT specimens and the complex K solution for wide specimens. In addition, John and Rigling [32] obtained another FEA results of the K factor that are also used in practice.

To understand the two K solutions used in BS 8571 [16] for clamped SENT specimens, Zhu [19] compared the analytical K solution obtained by Ahmad et al. [31] with three numerical K solutions obtained by Shen et al. [12], Cravero and Ruggieri [22] and John and Rigling [32], as shown in Fig. 2. It is seen that the analytical K solution of Ahmad et al. (used in BS 8571) agrees with the three numerical results for crack sizes up to a/W=0.6, and then deviates from the FEA results for all deep cracks when a/W>0.6. This implies that the K solution used by BS 8571: 2014 contains errors for the deep cracks of a/W>0.6.

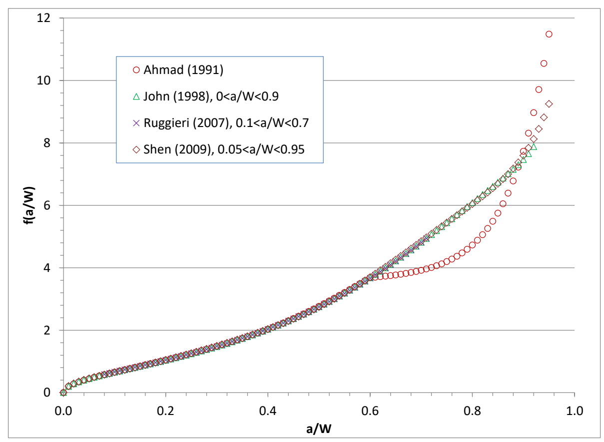

Figure 2. Comparison of analytical solution and numerical results for clamped SENT specimen, taken from [19]

Recall that the maximum valid crack size set in BS 8571 is a/W=0.6, and so the complex K solution used by BS 8571 for wide specimens has no effect on the toughness evaluation if all other requirements are met. However, use of a K solution containing errors in any fracture test standard is unacceptable. Thus, Zhu [19] restudied the analytical method used by Ahmad et al. [31], and obtained a corrected solution of the K factor for clamped SENT specimens over a large range of a/W.

More recently, Zhu [20] obtained a general full-range analytical solution of the K factor for the clamped SENT specimens with all possible H/W ratios as needed in a fracture or fatigue test. For the clamped SENT specimens with H/W=10, the following closed-form solution of the geometrical function, F, of the K factor was obtained using the regression method:

$$F(\alpha) = \frac{\alpha^{1/2}}{(1+2\alpha)(1-\alpha)^{3/2}} \left[\begin{array}{r} 1.9873 + 0.7422\alpha + 11.188\alpha^2 - 45.820\alpha^3 \\ +100.490\alpha^4 - 120.03\alpha^5 + 51.448\alpha^6 \end{array} \right] \quad (11)$$

Comparison with the numerical integration results shows that the 6th-order curve-fit function in Eq. (11) has a higher accuracy at 0.25% over $0 \le a/W \le 0.88$ and 0.5% over $0.88 < a/W < 0.97$.

Figure 3 compares the geometrical function of the full-range K solution in Eq. (11) with the corrected K solution obtained by Zhu [19] and three FEA results of the K factor obtained by John and Rigling [31] over 0≤a/W≤0.9, Cravero and Ruggieri [22] over 0.1≤a/W≤0.7 and Shen et al. [13] over 0.05≤a/W≤0.95. It shows that all numerical results match well with the corrected K solution and the full-range K solution. Note that all those K solutions are independent of specimen thickness B.

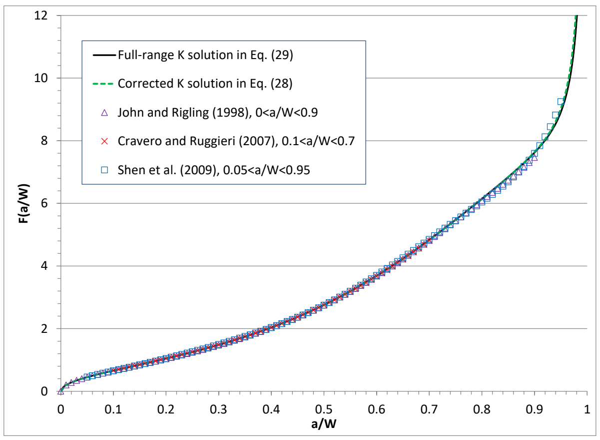

Figure 3. Comparison of the full-range K solution with the corrected K solution and three FEA results, taken from [20]

Figure 4 shows the relative errors of the corrected K solution and three numerical results in comparison to the full-range K solution. It is observed that the corrected K solution is very accurate over 0<a/W<0.90 with an error less than 0.30%, and the other numerical solutions are also accurate over 0.15≤a/W≤0.75 with an error less than 0.65% for the USP solution, 0.75% for John & Rigling's solution, and 0.72% for the CANMET solution. As a result, the full-range K solution is the most accurate to use, whereas the corrected K solution and three numerical K solutions are also adequate to use over the valid range for SENT testing.

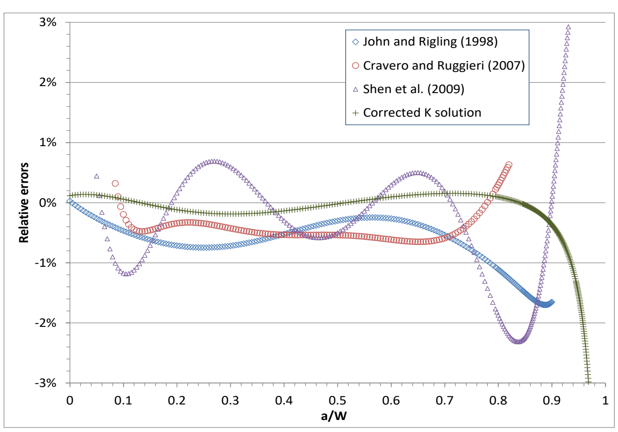

Figure 4. Relative errors of three FEA results compared with the full-range K solution, taken from [10]

Recently, Bassindale et al. [33] obtained a more accurate numerical solution of K using the FEA calculations for clamped SENT specimens with crack sizes covering a large range of 0.05≤a/W≤0.9. From their FEA results, those authors confirmed that the full-range K solution proposed by Zhu [20] is very accurate with a maximum error less than 0.23% over a large crack range of 0.2≤a/W≤0.7, and the CANMET results [13] are also sufficiently accurate with a maximum error less than 0.69% over the same crack range. As a result, those two K solutions can be used in the experimental evaluation of SENT testing.

3.2 Geometrical η Factors

DNV [11], CANMET [12-13] and USP [22-23] proposed different expressions of the geometrical eta (η) factors for clamped SENT specimens. Zhu [10] pointed out that there is no broad agreement over a large range of crack sizes, and the eta factor obtained by DNV [11] should not be used because of the complex expression and potential overestimation even in their validated range of a/W.

From the plane strain FEA simulations, Shen et al. [13], Ruggieri et al. [22, 23, 34] obtained the numerical solutions of the CMOD and load-line displacement (LLD) based eta factors (η_{CMOD} and η_{LLD}), where η_{CMOD} is used in Eq. (2) or Eq. (3), and η_{LLD} is used to determine the γ factor required in Eq. (3). Because the SENT specimen with a square cross-section is the central interest for developing a standard SENT test method, and thus these SENT specimens were employed by different investigators [34, 35] in the 3D FEA simulations to determine the expressions of the η factor.

Figure 5 compares the numerical results of the η_{CMOD} factor for clamped SENT specimens, where CANMET-Eq. (9), USP-Eq. (16), and USP-Eq. (17) denote the η_{CMOD} solution obtained by Shen et al. [13], Cravero and Ruggieri [22], and Mathias et al. [34], respectively, in addition to Ruggieri [23] and Huang and Zhou [35] for N=10. This figure was taken from Zhu [10], and so the equation number marked in Fig. 5 was used by Zhu [10], but not used in this paper.

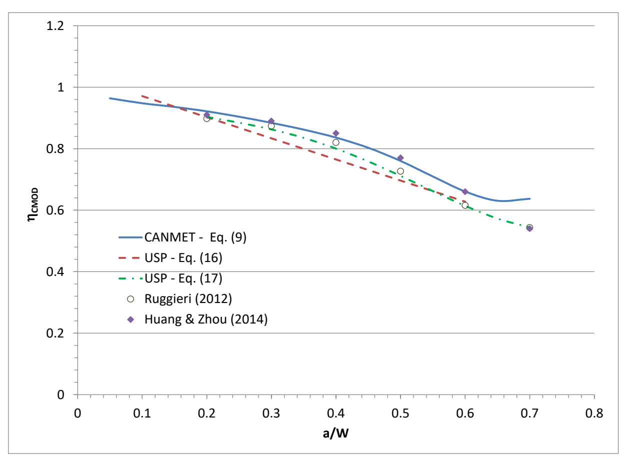

Figure 5. Comparison of available results of the η_{CMOD} factor, taken from [10]

Figure 5 shows that (a) the linear solution by Cravero and Ruggieri [22] is less accurate and should not be used, (b) the CANMET solution is adequate to use over 0.05<a/W<0.65 because it matches the FEA results by Huang and Zhou [35], and (c) the USP solution by Mathias et al. [34] is appropriate to use over a larger range of 0.2≤a/W≤0.7 because it closely matches with the FEA results obtained by Ruggieri [23]. Therefore, the solution of η_{CMOD} [34] is recommended for use:

$$\eta_{CMOD} = 1.067 - 1.767\alpha + 7.808\alpha^2 - 18.269\alpha^3 + 15.295\alpha^4 - 3.083\alpha^5 \quad (12)$$

Figure 6 compares the numerical curve-fit solutions of the η_{LLD} factor obtained by Shen et al. [13] (or CANMET in Eq. (9)) and by Mathias et al. [34] (or USP in Eq. (17)). This figure was taken from Zhu [10], and so the equation number marked in this figure was used by Zhu [10]. Also included in Fig. 6 are three FEA results obtained by Ruggieri [23], Huang and Zhou [35] and Mercier [36] for clamped SENT specimens with N=10. It is observed that (a) the CANMET solution is more accurate in its valid range because it agrees well with FEA results of Ruggieri [23] and Mercier [36], (b) the USP solution by Mathias et al. [34] is close to the CANMET solution with slight conservatism, and (c) the FEA results obtained by Huang & Zhou [35] is inaccurate because they are much higher than the other FEA results over a large range. Therefore, both CANMET and USP η_{LLD} solutions are adequate to use over the range of 0.1≤a/W≤0.7. Due to slight conservatism, the USP solution [34] is recommended for use:

$$\eta_{LLD} = -0.623 + 9.336\alpha - 4.584\alpha^2 - 47.963\alpha^3 + 87.697\alpha^4 - 44.875\alpha^5 \quad (13)$$

Although the USP solutions of two geometrical η factors in Eqs (12) and (13) are recommended, the CANMET solutions of the η factors are also acceptable for practical use. Nevertheless, further FEA simulations could be needed for obtaining more accurate results of these two η factors.

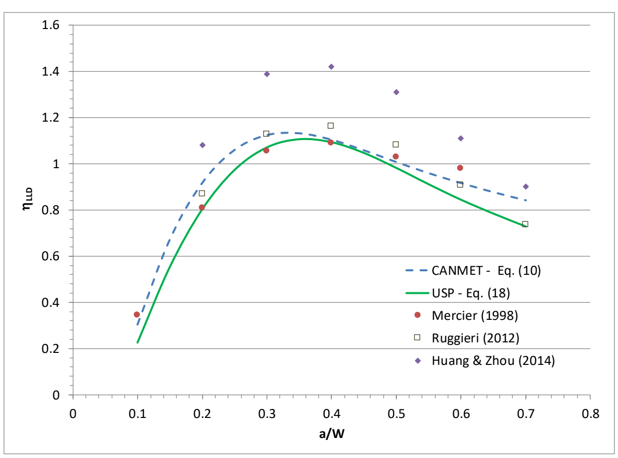

Figure 6. Comparison of available solutions of the η_{LLD} factor, taken from [10]

3.3 CMOD Compliance and Inverse Equation

As well recognized, the unloading compliance technique is an effective approach to monitor crack length for a single SENT specimen test. With CMOD and its compliance measurements, crack extension can be estimated using an adequate compliance equation. Various compliance equations have been proposed for clamped SENT specimens, including the CANMET solution by Shen et al. [13], the USP solution by Cravero and Ruggieri [22] or Mathias [35] and many others. Tyson et al. [37] reported more accurate FEA results of CMOD compliance. After comparison, Zhu [10] pointed out that both CANMET and USP solutions are adequate to use. The CANMET solution of CMOD compliance inverse equation was obtained by Shen et al. [13]:

$$\frac{a}{W} = 2.072 - 16.411u + 79.600u^2 - 211.670u^3 + 236.857u^4 + 27.371u^5 - 179.740u^6 - 86.280u^7 + 171.764u^8 \quad (14)$$

and the USP solution of CMOD compliance inverse equation was obtained by Cravero and Ruggieri [22]:

$$\frac{a}{W} = 1.6485 - 9.1005u + 33.025u^2 - 78.467u^3 + 97.344u^4 - 47.227u^5 \quad (15)$$

The comparison in Zhu [10] with the more accurate FEA results obtain by Tyson et al. [37] shows that Eq. (14) has an accuracy of -0.36% over 0.05≤a/W≤0.9, and Eq. (15) has an accuracy of 0.26% over 0.1≤a/W≤0.8.

More recently, the present author [38] obtained an analytical solution of CMOD compliance equation that is consistent with the full-range K solution for the clamped SENT specimen. For the clamped SENT specimens with H/W=10, the full-range CMOD compliance equation was obtained as:

$$EBC_{cmod} = \frac{2\alpha}{(1-\alpha)^2}(2.9168 - 5.7135\alpha + 14.213\alpha^2 - 20.736\alpha^3 + 23.209\alpha^4 - 29.019\alpha^5 15.132\alpha^6) \quad (16)$$

where α=a/W, E is the Young's modulus, C_{cmod} is compliance.

Figure 7 compares the CMOD compliance solutions in Eq. (16) with other available solutions and FEA data for clamped SENT specimens, where the numerical results were obtained by CANMAT [13], Cravero and Ruggieri [22], Souza and Ruggieri [39], and Fonzo et al. [40], respectively. The FEA data obtained by John and Rigling [32] and Tyson et al. [37] are also included in this figure for comparison. It shows that the new compliance equation (16) matches well with the existing numerical solutions up to a/W=0.85, and then starts to deviate from those results. This implies that the new CMOD compliance equation may overestimate the compliance for very deep cracks of a/W>0.85. Based on this, it is concluded that the new CMOD compliance equation (16) is very accurate for crack sizes up to a/W=0.85. And thus, this simple CMOD compliance equation (16) is adequate to use for estimating CMOD compliance if the unloading compliance technique is utilized for a single SENT specimen test in the end-clamped conditions.

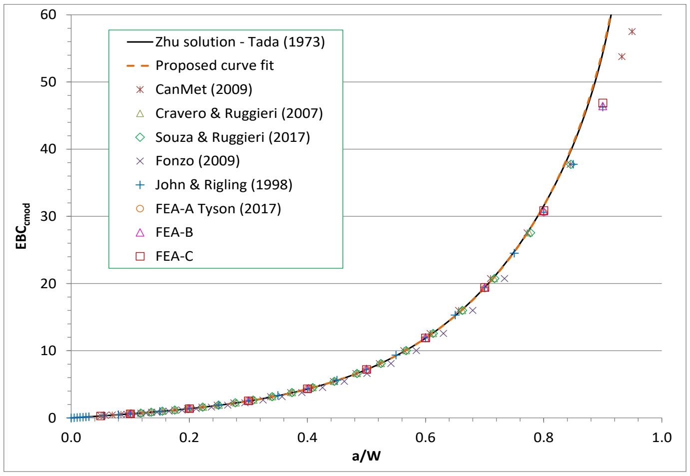

Figure 7. Comparisons of CMOD compliance of proposed solution with other available solutions and FEA data

From Eq. (16), the CMOD compliance inverse equation is expressed in a fifth-order polynomial function as:

$$\frac{a}{W} = 1.4747 - 6.3559u + 16.404u^2 - 30.563u^3 + 31.653u^4 - 12.79u^5 \quad (17)$$

where $u = 1/(\sqrt{BEC} + 1)$ is the normalized compliance for the plane stress conditions. The Young's modulus E is replaced using $E' = E/(1-\nu^2)$ for the plane strain conditions. Figure 8 compares the proposed solution with the numerical results of the inverse equation, and shows that the CMOD compliance inverse equation (17) is very accurate over the wide range of 0<a/W<0.9.

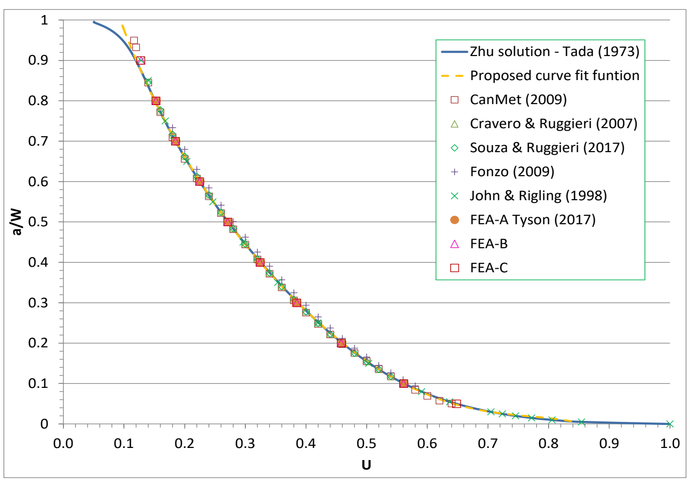

Figure 8. Comparisons of the proposed CMOD compliance reverse solution with numerical solutions and FEA data

The m Factor for Converting J to CTOD

3.4 The m factor

As discussed previously, two different methods were developed for determining CTOD and its R-curves for SENT specimens. One is the J-integral conversion method, and the other is the DCG measurement method. For the J-integral conversion method, the key is to obtain an accurate solution of the m factor required in Eq. (4). The CANMET procedure developed a loading-dependent m factor, as given in Eqs (5) and (6). In contrast to this, many other researchers [26-28] developed numerical results for loading-independent m factors.

Using experimental test data recently obtained at EWI for a low strain hardening steel (X80) and a high strain hardening steel (A36), Zhu et al. [30] evaluated five available m factors for a large range of crack extension for both X80 and A36 steels. Figure 9 shows the variation of five available m factors with the crack extension expressed as the a/W ratio for the pipeline steel X80 and the structural steel A36, where the references marked in Fig. 9 were given in Reference [30]. From these figures, similar trends and large scatters are observed for those m factors. For the loading-dependent m factor, as given in Eqs (5) and (6), after crack initiation, the m factor increases with crack extension, but has no physical meaning after a/W=0.5 because CANMET only used the FEA results at a/W=0.2 and a/W=0.5 for the curve-fitting. For the four loading-independent m factors, all results of the m factor keep nominally constant during the crack extension, and the 3D results are larger than the 2D results. Without further study, it is difficult to determine which is better. Thus, the m factor as given in Eq. (7) obtained by Sarzosa et al. [27] using the 3D FEA simulations for side-grooved specimens was suggested by Zhu [10] and Ruggieri [28] for practical use in order to obtained conservative CTOD-R curves.

(a)

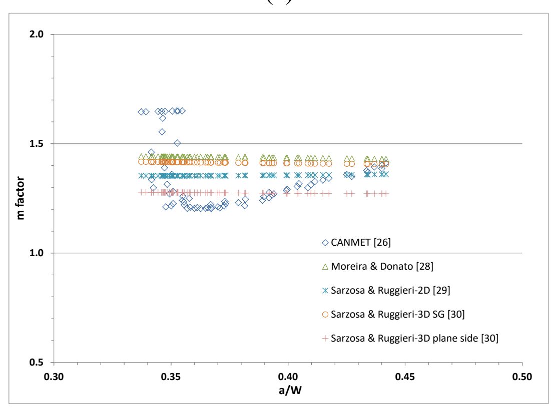

(b)

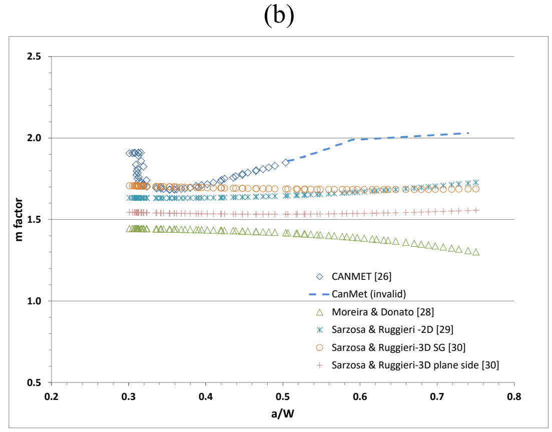

Figure 9. Comparison of five available m factors for (a) X80 and (b) A36, taken from [30]

3.5 Comparison of J-Converted and DCG measured CTOD

There are three DCG test methods available for the SENT CTOD testing, i.e., the ExxonMobil total CTOD method [14], the UGent total CTOD method [29], and the BS 8571 separated CTOD method [16]. Experimental results of Zhu et al. [30] showed that these three DCG methods determined comparable CTOD results and CTOD-R curves for both X80 and A36 steels, and thus all three DCG test methods are adequate to use for developing a CTOD-R curve from a single-specimen SENT test. However, BS 8571 CTOD method is preferred to use because it is consistent with the definition of CTOD in ASTM E1820 [18] and determines slightly conservative CTOD.

In contrast to the DCG methods, the J-conversion method with different m factor solutions can determine similar or different CTOD-R curves. Figures 10(a) and 10(b) compare the CTOD-R curves from the J-conversion method with three selected *m* factors that were obtained by CANMET in Eq. (5), Huang & Zhou [25], and Sarzosa et al. [27], respectively for X80 and A36 steels. The total CTOD-R curves obtained using the ExxonMobil method these two steels are also included in Fig. 10 for comparison. As evident from these figures, the ExxonMobil method works fine for X80 steel for a short crack extension, but does not work for A36 steel because this method considerably overestimates the CTOD-R curve for A36 steel.

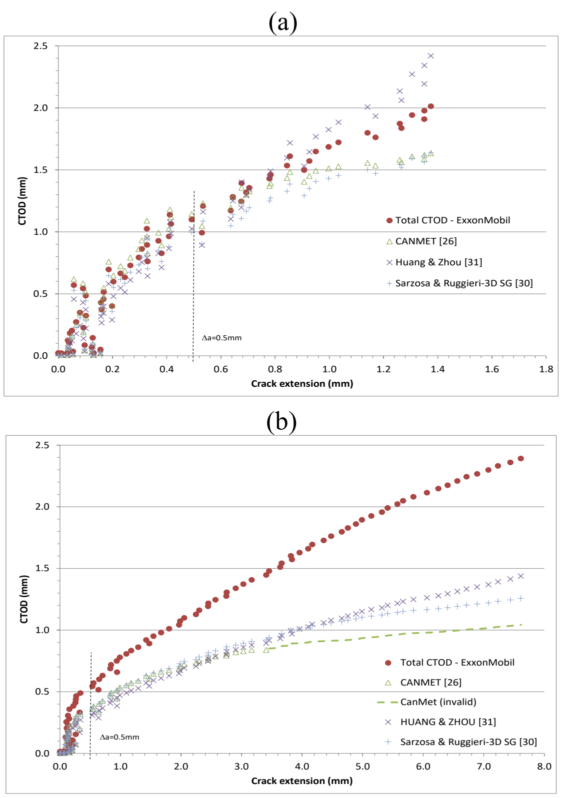

Figure 10. Comparisons of CTOD-R curves obtained by J-conversion methods for (a) X80 and (b) A36, taken from [30]

Moreover, Figure 10(a) shows that the three m factors determine comparable CTOD-R curves for small crack extensions less than 1.0 mm, but Huang and Zhou determine unrealistically high results for larger crack extensions for X80 steel. Figure 10(b) shows that the three m factors determine comparable CTOD-R curves for the crack extension up to 3.5 mm for A36 steel, and then deviate gradually for larger crack extensions where the CAMET m factor breakdowns (because the m factor is valid for $0.2 \le a/W \le 0.5$). Due to these observations, the USP m factor in Eq. (7) is recommended for practical use in the SENT fracture testing for determining a conservative CTOD-R curve for ductile steels.

4 SENT Fracture Test methods for Pipeline Welds

The above-discussed test methods and estimate equations were developed for base steels, but not for weldments. In fact, different investigators [34, 41-45] have studied the SENT test methods for weld materials and the effect of mismatch level and weld width on the J-integral and CTOD calculations. Different equations of the eta and m factors were proposed. Recently, Afzalimir et al. [44] presented a summarized studies on this topic and provided the following equations of the eta and m factors for a typic X80 weldment with a mismatch ratio of 1.18.

$$\eta_{J-CMOD} = 0.950 + 0.622\left(\frac{a}{W}\right) - 4.099\left(\frac{a}{W}\right)^2 + 3.548\left(\frac{a}{W}\right)^3 \quad (18)$$

$$\eta_{J-LLD} = 1.646 - 10.023\left(\frac{a}{W}\right) + 57.288\left(\frac{a}{W}\right)^2 - 141.889\left(\frac{a}{W}\right)^3 + 153.709\left(\frac{a}{W}\right)^4 - 60.667\left(\frac{a}{W}\right)^5 \quad (19)$$

$$m = 1.256 - 0.129\left(\frac{a}{W}\right) - 0.068\left(\frac{a}{W}\right)^2 - 0.071\left(\frac{a}{W}\right)^3 \quad (20)$$

The comparisons [34, 44] showed that Eqs. (18)-(20) of the eta and m factors for the X80 weld are very close to those for the X80 steel, and both J-R and CTOD-R curves for the weld and base steel have slight differences with lower values for the weld.

5 IMPROVED SENT FRACTURE TEST METHOD

Based on the above analyses and comparisons, an improved SENT fracture test method is proposed here for determining J-R curves and CTOD-R curves using clamped SENT specimens.

5.1. SENT Test Method for Measuring J-R Curves

Following the guideline of ASTM E1820, the J-integral is separated into an elastic component J_{el} and a plastic component J_{pl}, as shown in Eq. (1). The elastic J_{el} is determined from the stress intensity factor K using $J_{el}=K^2/E'$, and the plastic J_{pl} is calculated from the eta equation (2) if the one-point toughness J_{IC} is needed, or from the CMOD-based incremental J-integral equation (3) if a J-R curve is desired to develop using the clamped SENT specimens.

To complete the calculation for the J-integral, in addition to use of measured applied force P and CMOD data, one needs the K factor solution, CMOD-based geometrical factor η_{CMOD}, LLD-based geometrical factor η_{LLD} that is used to calculate the γ factor required in Eq. (3), and CMOD compliance inverse equation used to estimate crack length during crack tearing. Based on the previous studies, the best or more accurate solutions of these four quantities are proposed as follows.

1). The K factor solution is given in Eq. (11) or the full-range solution that was developed by Zhu [20].

2). The η_{CMOD} and η_{LLD} factors are expressed in Eqs (12) and (13) that were obtained by Mathias et al. [34].

3). The CMOD compliance inverse equation is described by Eq. (17) that was recently proposed by Zhu [38].

Alternatively, some solutions of the four quantities that have similar accuracy can be used in the calculation of the J-integral. Those include the CANMET K solution [13] or the USP K solution [22], the CANMET η_{CMOD} and η_{LLD} solutions [13], and the CANMET compliance inverse equation (14) or the USP compliance inverse equation (15). Further experimental data for different pipeline steels are needed to assess the differences in evaluation of J-R curves using those solutions.

5.2. SENT Test Method for Measuring CTOD-R Curves

As similar to ASTM E1280, this paper recommends the J-integral conversion method for determining CTOD from Eq. (4), where the m factor is described by Eq. (7) or the USP solution that was obtained by Sarzosa et al. [27]. If a CTOD-R curve is needed to develop, crack length should be estimated using the CMOD compliance equation (17) that was proposed by Zhu [38].

5.3 A Challenge for Determining CTOD Toughness

As discussed earlier, there are two CTOD definitions. One is the J converted CTOD, as just recommended above, and the other is DCG measured CTOD, as defined by BS 8571 in Eq. (10). These two CTOD methods may determine comparable values of CTOD toughness for some steels, but significantly different values for other steels, as shown next.

Figures 11(a) and 11(b) compare experimental CTOD-R curves determined using the J-integral conversion method and the DCG measurement method, respectively for X80 and A36 steels, where the J-conversion method uses the proposed J-R curve procedures and the USP m factor in Eq. (7), and the DCG method uses Eq. (10) as prescribed in BS 8571.

For the low strain hardening steel X80, Fig. 11(a) shows that (1) the J-conversion and DCG methods determine comparable initiation CTOD up to crack extension of 0.5 mm (a nominal crack initiation), and (2) the two R-curves deviate from each other at this crack initiation, and the DCG measured curve is gradually higher than the J-converted curve, with an increasing difference with crack extension. The similar observations were reported by Weeks et al. [46-47] for X100 pipeline steel and by Park et al. [48-49] for X70 pipeline steel and its welds.

For the high strain hardening steel A36, Fig. 11(b) shows that the J-conversion and DCG methods determine two significantly different CTOD-R curves over the entire crack growth, including the crack initiation. Particularly, the DCG method determines remarkably high nominal initiation toughness and CTOD-R curve in comparison to those determined by the J-converted CTOD method.

(a)

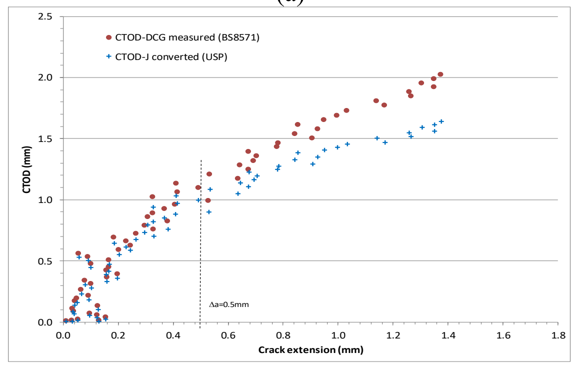

(b)

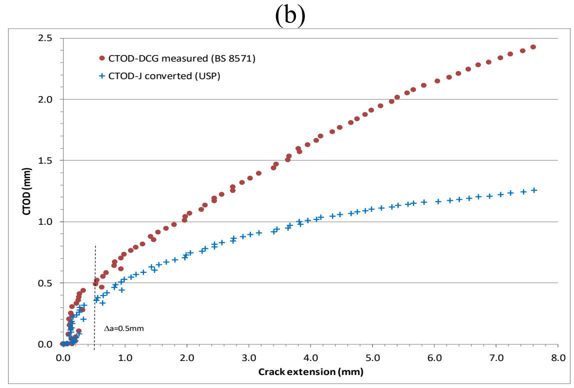

Figure 11. Comparisons of CTOD-R curves determined using J-conversion and DCG methods (a) X80, and (b) A36

Recently using the numerical analysis, Zhu and McGaughy [50] investigated the root causes of the large difference between the DCG measured and J-converted CTOD values for X80 and A36 steels. However, this topic remains a big challenge, and needs to be further studied.

6 CONCLUSIONS

This paper presented a comparative study on the primary available SENT test methods for measuring less-conservative fracture toughness, including CANMET method, ExxonMobil method and BSI 8571 standard method in terms of the J-integral and CTOD. Detailed comparisons were made for the stress intensity factor, the geometrical eta factors, the CMOD compliance inverse equation, and the m factor used in the J-converted method to calculate CTOD. The weld effect on the fracture test method was also discussed. On these bases, an improved SENT fracture toughness test method was proposed for determining reliable J-R curves and/or CTOD-R curves. The following conclusions are obtained:

(1). The full-range K solution in Eq. (11) is very accurate and recommended for use in calculation of the elastic J-integral. The CANMET K solution in [13] and the USP K solution in [22] are also accurate in the range of $0.2 \leq a/W \leq 0.7$ and adequate to use in practical SENT testing.

(2). The solutions of the geometrical eta factors developed by CANMET [13] and USP [34] are acceptable for practical use in SENT testing. Equations (12) and (13) are recommended for use due to their slight conservatism.

(3). The wide-range solution of CMOD compliance inverse equation [17] is very accurate to use. In addition, the CANMET and USP CMOD elastic compliance equations (14) and (15) are also accurate to use for estimating crack extension when the unloading compliance technique is employed in SENT testing.

(4). Large differences and big scatters exist between the existing solutions of the m factor, resulting in inconsistent CTOD-R curves for the same steel. Further study is needed.

(5). Differences between the CTOD-R curves determined using the J-conversion method and the DCG measurement are relatively small for low-hardening steels (like X80), but become significantly large for high-hardening steels (like A36). This is a big challenge, and further studies are needed for appropriately understanding and solving this problem.

REFERENCES

[1] Irwin GR. "Analysis of stresses and strains near the end of a crack traversing a plate," *Journal of Applied Mechanics*, Vol. 24, 1957: 361-164.

[2] Rice JR. "A path independent integral and the approximate analysis of strain concentrations by notches and cracks," *Journal of Applied Mechanics*, Vol. 35, 1968: 379-386.

[3] Wells AA. "Application of fracture mechanics at and beyond general yielding," *British Welding Journal*, Vol.10, 1963: 563-570.

[4] API 579 (or ASME FFS-1 2007), *Fitness for Service*, American Petroleum Institute, Washington DC, 2007.

[5] BS 7910: 2013 +A1: 2015, *Guide to Methods for Assessing the Acceptability of Flaws in Metallic Structures*, British Standards Institution, December 2013.

[6] Zhu XK, Joyce JA. "Review of fracture toughness (G, K, J, CTOD, CTOA) testing and standardization," *Engineering Fracture Mechanics*, Vol. 85, 2012: 1-46.

[7] Zhu XK. "Review of fracture toughness test methods for ductile materials in low - constraint conditions," *International Journal of Pressure Vessels and Piping*, Vol. 139-140, 2016: 173-183.

[8] Zhu XK, Leis BN. "Application of constraint-corrected J-R curve to fracture analysis of pipelines," *Journal of Pressure Vessel and Technology*, Vol. 128, 2006: 581-589.

[9] Zhu XK, McGaughy T. "Development of Fracture Toughness Testing and Evaluation Using SENT Specimens," *Proceedings of the 10th International Pipeline Conference*, Calgary, Alberta, Canada, September 29 – October 3, 2014.

[10] Zhu XK. "Progress in Development of Fracture Toughness Test Methods for SENT Specimens," *International Journal of Pressure Vessels and Piping*, Vol. 156, 2017: 40-58.

[11] DNV, 2006, *Recommended Practice DNV-RP-F108: Fracture Control for Pipeline Installation Methods Introducing Cyclic Plastic Strain*, Det Norske Veritas, Norway.

[12] Shen G, Gianetto JA, Tyson WR., 2008, *Development of Procedure for Low-Constraint Toughness Testing Using a Single-Specimen Technique*, MTL Report No. 2008-18(TR).

[13] Shen G, Gianetto JA, Tyson WR. "Measurement of J-R Curves Using Single-Specimen Technique on Clamped SE(T) Specimens," *Proceedings of 18th International Offshore and Polar Engineering Conference*, Osaka, Japan, June 21-26, 2009.

[14] ExxonMobil Upstream Research Company, 2010, *Measurement of Crack-Tip Opening Displacement (CTOD) Fracture Resistance Curves Using Single-Edge Notched Tension (SENT) Specimen*, September 20, 2010.

[15] Tang H, Macia M, Minnaar K, Gioielli P, Kibey S., Fairchild D., "Development of the SENT Test for Strain-Based Design of Welded Pipelines," *Proceedings of the 8th International Pipeline Conference*, Calgary, Canada, September 27 - October 1, 2010.

[16] BS 8571, 2014, *Method of Test for Determination of Fracture Toughness in Metallic Materials Using Single Edge Notched Tension (SENT) Specimens*, British Standards Institution.

[17] Zhu XK, Weeks TW. A Special Issue on SENT Fracture Toughness Testing and Its Applications to High-Strength Pipelines, *International Journal of Pressure Vessels*, Vol. 156, September 2017.

[18] ASTM E1820-18, 2018, *Standard Test Method for Measurement of Fracture Toughness*, American Society for Testing and Materials International.

[19] Zhu XK. "Corrected Stress Intensity Factor Solution for A British Standard Single Edge Notched Tension (SENT) Specimen," *Fatigue & Fracture of Engineering Materials & Structures*, Vol. 39, 2016: 120-131.

[20] Zhu XK. "Full-range Stress Intensity Factor Solutions for Clamped SENT Specimens," *International Journal of Pressure Vessels and Piping*, Vol. 149, 2017: 1-13.

[21] Zhu XK, Leis BN, Joyce, JA. "Experimental Estimation of J-R Curve from Load-CMOD Records for SE(B) Specimens," *Journal of ASTM International*, Vol. 5, 2007, Paper ID: JAI101532.

[22] Cravero S, Ruggieri C. "Estimation procedure of J-Resistance curves for SE(T) fracture specimens using unloading compliance," *Engineering Fracture Mechanics*, 2007; 74: 2375-2757.

[23] Ruggieri C. "Further results in J and CTOD estimation procedures for SE(T) fracture specimens – Part I: homogeneous materials," *Engineering Fracture Mechanics*, Vol. 79, 2012: 245-265.

[24] Shen G, Tyson WR. "Evaluation of CTOD from J-integral for SE(T) specimens", *Proceedings of Pipeline Technology Conference*, Ostend, Belgium, October 7-9, 2009.

[25] Huang Y, Zhou W. "J-CTOD Relationship for Clamped SE(T) Specimens based on Three-Dimensional Finite Element Analyses," *Engineering Fracture Mechanics*, Vol. 131, 2014: 643-655.

[26] Moreira F, Donato G. "Estimation procedure for J and CTOD fracture parameter experimental evaluation using homogenous and mismatched clamped SE(T) specimens," *Proceedings of ASME Pressure Vessel & Piping Conference*, Bellevue, WA, USA, July 18-22, 2010.

[27] Sarzosa DFB, Souza RF, Ruggieri C. "J-CTOD Relations in Clamped SE(T) Fracture Specimens Including 3D Stationary and Growth Analysis," *Engineering Fracture Mechanics*, Vol. 147, 2015, pp. 331-354.

[28] Ruggieri C. "Low Constraint Fracture Toughness Testing Using SE(T) and SE(B) specimens," *International Journal of Pressure Vessels and Piping*, Vol. 156, 2017: 40-58.

[29] Verstraete M, Hertelé S, Minnebruggen KV, Denys R, Waele WD. "UGent Guidelines for SENT Testing," *Proceedings of the 6th International Pipeline Technology Conference*, Ostend, Belgium, October 6-9, 2013.

[30] Zhu XK, Zelenak P, McGaughy T. "Comparative study of CTOD-Resistance curve test methods for SENT specimens," *Engineering Fracture Mechanics*, Vol. 172, 2017, pp. 17-38.

[31] Ahmad J, Papaspyropoulos V, Hopper AT. "Elastic-plastic analysis of edge-notched panels subjected to fixed grip loading," *Engineering Fracture Mechanics*, Vol. 38, 1991: 283-294.

[32] John R, Rigling B. "Effect of height to width ratio on K and CMOD solutions for a single edge cracked geometry with clamped ends," *Engineering Fracture Mechanics*, Vol. 60, 1998: 147-156.

[33] Bassindale C, Wang X, Tyson WR, Xu S. "Numerical versification of stress intensity factor solution for clamped single edge notched tension (SENT) specimens," *Fatigue & Fracture in Engineering Materials and Structures*, Vol. 41, 2018: 494-499.

[34] Mathias LLS, Sarzosa DFB, Ruggieri C. "Effects of specimen geometry and loading mode on crack growth resistance curves of a high-strength pipeline girth weld," *International Journal of Pressure Vessels and Piping*, Vol. 111-112, 2013: 106-119.

[35] Huang Y, Zhou W. Investigation of plastic eta factors for clamped SE(T) specimens based on three-dimensional finite element analyses, *Engineering Fracture Mechanics*, 2014; 132: 120-135.

[36] Mercier GP. *Elastic and Plastic Analysis of a Single Edge Cracked Tension Specimen with Clamped Ends*, Technical Report NSWCCD-61-TR-1998/27, Naval Surface Warfare Center, October 1998.

[37] Tyson WR, Ruggieri C, Zhou W, Wang E. Effective modulus for crack size measurement with SE(T) specimens using unloading compliance, *Journal of Testing and Evaluation*, Vol. 45, 2017, JTE20150488.

[38] Zhu XK. "A Wide Range Solution of CMOD Compliance for Clamped SENT Specimens," *Proceedings of ASME Pressure Vessels and Piping Conference*, July 19-24, 2020; Virtual, Online.

[39] de Souza RF, Ruggieri C. "Revised Wide Range Compliance Solutions for Selected Standard and Nonstandard Fracture Test Specimens based on Crack Mouth Opening Displacement," *Engineering Fracture Mechanics*, Vol. 179, 2017: 77-92.

[40] Fonzo A, Melis G, Di Vito G, Mannucci G. "Measurement of Fracture Resistance of Pipelines for Strain Based Design," *Proceedings of the 17th PRCI-EPRG-APIA Jointed Technical Meetings on Pipeline Research*, Milan, Italy, May 11-15, 2009.

[41] Paredes M, Ruggieri C. "Further results in J and CTOD estimation procedures for SE(T) fracture specimens – Part II: Weld centerline cracks." *Engineering Fracture Mechanics*, 2012; 89: 24-39.

[42] Ruggieri C, Sarzosa DFB, Hippert E. "Fracture resistance testing of pipeline girth welds with strength undermatch using low-constrain specimens." *Procedia Structural Integrity*, 2019; 18: 36-45.

[43] Jia P, Jiang W, Zhan S, Zhao X. "Estimation of plastic eta factor for clamped-end SE(T) specimens with undermatched weld metal based on 3D finite element analysis," *Theoretical and Applied Fracture Mechanics*, 2020; 106: 102496.

[44] Afzalimir SH, Barbosa VS, Ruggieri C. "Evaluation of CTOD resistance curves in clamped SE(T) specimens with weld centerline cracks." *Engineering Fracture Mechanics*, 2020; 240: 107326.

[45] Li Z, Gong B, Lacidogna G, Deng C, Wang D. "Strain-based fracture response of X80 steel pipe welded girth based on constraint-modified J-R curves: from SENT specimen to full-scale pipe." *Engineering Fracture Mechanics*, 2021, 258: 108114.

[46] Weeks TS, Lucon E, "Direct Comparison of Single Specimen Clamped SE(T) Test Methods on X100 Line Pipe Steel," *Proceedings of the 10th International Pipeline Conference*, Calgary, Canada, Sept 29-Oct 3, 2014.

[47] Weeks TS, Read DT, "Comparison of J-integral from Single Specimen SE(T) Tests on API-5L X100 Line Pipe Steel," *Proceedings of the 25th ISOPE Conference*, Kona, Hawaii, June 21-26, 2015.

[48] Park DY, Gravel JP, Simha, CHM, Liang J, Duan DM. "Low-Constraint Toughness Testing of Two SE(T) Methods in a Single Specimen," *Proceedings of ASME Pressure Vessel and Piping Conference*, Anaheim, California, July 20-24, 2014.

[49] Park DY, Gravel JP, Arafin M, Liang J, Simha CHM. "Evaluation of Two Low-Constraint Toughness Test Methods in a Single Specimen," *Journal of Engineering Material Technology*, Vol. 137, 2014, 011003.

[50] Zhu XK, McGaughy T. "CTOD-Resistance Curve Testing and Evaluation for Clamped SENT Specimens," *Proceedings of the 12th International Pipeline Conference,* Calgary, Canada, September 24-28, 2018.